Atmos. Chem. Phys., 15, 1289–1298, 2015
www.atmos-chem-phys.net/15/1289/2015/
doi:10.5194/acp-15-1289-2015

Atmospheric Chemistry and Physics Open Access

Evidence for an unidentified non-photochemical ground-level source of formaldehyde in the Po Valley with potential implications for ozone production

J. Kaiser[1], G. M. Wolfe[1,*,], B. Bohn[2], S. Broch[2], H. Fuchs[2], L. N. Ganzeveld[3], S. Gomm[2], R. Häseler[2], A. Hofzumahaus[2], F. Holland[2], J. Jäger[2], X. Li[2], I. Lohse[2], K. Lu[2,***], A. S. H. Prévôt[4], F. Rohrer[2], R. Wegener[2], R. Wolf[4], T. F. Mentel[2], A. Kiendler-Scharr[2], A. Wahner[2], and F. N. Keutsch[1]**

[1]Chemistry, University of Wisconsin-Madison, Madison, WI, USA
[2]Institut für Energie- und Klimaforschung Troposphäre IEK-8, Forschungszentrum Jülich GmbH, Jülich, Germany
[3]Earth System Science and Climate Change, Wageningen University and Research Center, Wageningen, Netherlands
[4]Laboratory of Atmospheric Chemistry, Paul Scherrer Institute, Villigen, Switzerland
[*]now at: Joint Center for Earth Systems Technology, University of Maryland Baltimore County, Baltimore, MD, USA
[**]now at: Atmospheric Chemistry and Dynamics Laboratory, NASA Goddard Space Flight Center, Greenbelt, MD, USA
[***]now at: College of Environmental Sciences & Engineering, Peking University, Beijing, China

Correspondence to: F. N. Keutsch (keutsch@chem.wisc.edu)

Received: 18 July 2014 – Published in Atmos. Chem. Phys. Discuss.: 1 October 2014
Revised: 19 December 2014 – Accepted: 12 January 2015 – Published: 6 February 2015

Abstract. Ozone concentrations in the Po Valley of northern Italy often exceed international regulations. As both a source of radicals and an intermediate in the oxidation of most volatile organic compounds (VOCs), formaldehyde (HCHO) is a useful tracer for the oxidative processing of hydrocarbons that leads to ozone production. We investigate the sources of HCHO in the Po Valley using vertical profile measurements acquired from the airship Zeppelin NT over an agricultural region during the PEGASOS 2012 campaign. Using a 1-D model, the total VOC oxidation rate is examined and discussed in the context of formaldehyde and ozone production in the early morning. While model and measurement discrepancies in OH reactivity are small (on average $3.4 \pm 13\,\%$), HCHO concentrations are underestimated by as much as 1.5 ppb (45 %) in the convective mixed layer. A similar underestimate in HCHO was seen in the 2002–2003 FORMAT Po Valley measurements, though the additional source of HCHO was not identified. Oxidation of unmeasured VOC precursors cannot explain the missing HCHO source, as measured OH reactivity is explained by measured VOCs and their calculated oxidation products. We conclude that local direct emissions from agricultural land are the most likely source of missing HCHO. Model calculations demonstrate that radicals from degradation of this non-photochemical HCHO source increase model ozone production rates by as much as $0.6\,\mathrm{ppb\,h^{-1}}$ (12 %) before noon.

1 Introduction

Stagnant air masses, abundant solar radiation, and high anthropogenic emissions make northern Italy's Po Valley one of Europe's most polluted regions. Previous measurements have shown that the regional O_3 background can reach as high as 90 ppb (Liu et al., 2007). Photochemical ozone production is tied to the reactions of NO_x ($NO + NO_2$), HO_x ($OH + HO_2$), and volatile organic compounds (VOCs). In the troposphere, NO_2 photodissociates to form oxygen atoms (Reaction 1), which then react with molecular oxygen to generate O_3 (Reaction 2). The partitioning of NO_x between NO and NO_2 determines the production rate of O_3. The hydroxyl-radical (OH) initiated oxidation of VOCs creates peroxy radicals ($XO_2 = HO_2 + RO_2$) (Reaction 3). These radicals shift the partitioning of NO_x radicals towards NO_2 (Reaction 4), thus increasing the net ozone production rate.

$$NO_2 + h\nu \rightarrow NO + O \quad \text{(R1)}$$

$$O + O_2 \rightarrow O_3 \quad \text{(R2)}$$

$$OH + VOC \rightarrow nXO_2 + \text{oxidized VOC} \quad \text{(R3)}$$

$$NO + XO_2 \rightarrow NO_2 + XO \quad \text{(R4)}$$

In this analysis, we define the net ozone production rate ($P(O_3)$) as the calculated difference between the NO_2 photolysis rate (Reaction 1) and the rate of NO to NO_2 conversion by O_3.

While measuring all VOCs and their oxidation products is non-trivial, formaldehyde (HCHO) is formed in the oxidation of nearly every VOC and thus provides a downstream constraint on this chemistry. In addition, photolysis of HCHO constitutes an important source of HO_2 radicals without consuming OH, effectively accelerating O_3 production via Reaction (4), followed by reactions (1) and (2).

In 2002–2003, the FORMAT (FORMaldehyde as A Tracer of oxidation in the troposphere) campaign aimed to use HCHO to trace the effect of VOC oxidation on ozone production in the Po Valley. Though modeling efforts focused primarily on the Milan urban plume, an agricultural region upwind of the city was also investigated in the 2003 FORMAT study (Liu et al., 2007). There, HCHO mixing ratios were up to 2 times higher than those predicted by regional chemistry transport models. Primary emissions were estimated to be a minor source of HCHO in the agricultural region ($\sim 10\,\%$), and OH-initiated oxidation of underrepresented local biogenic or anthropogenic VOC emissions was cited as the likely cause of underpredicted HCHO. Because the morning increase in HCHO was not well represented, and because the regional background was not well understood, the effect of anthropogenic emissions on the diurnal cycle under polluted conditions could not be reproduced by the model (Junkermann, 2009).

While HCHO measurements provide a product-based view of VOC oxidation, direct measurements of OH reactivity, the inverse lifetime of OH, can provide further insight into the instantaneous VOC oxidation rate. OH reactivity is calculated as

$$\text{OH reactivity } (s^{-1}) = \sum_i k_{X_i+OH}[X_i], \quad (1)$$

where k_{X_i+OH} are the rate coefficients for the reaction of all species X with OH. Field measurements of OH reactivity have been available since 2001, and Edwards et al. (2013) and Lou et al. (2010) provide summaries of recent comparisons of modeled and measured reactivity in a variety of environments. Notably, measurements in Paris demonstrated that more than half of the measured reactivity in highly aged continental air masses could not be explained by available measurements (Dolgorouky et al., 2012). The authors concluded that the missing OH sink was likely (multi)oxidized compounds from processed anthropogenic emissions. Previous work has examined the effect of discrepancies between modeled and measured OH reactivity on calculated O_3 production potentials (Sadanaga et al., 2005; Yoshino et al., 2012). In one study in Tokyo, including unmeasured VOC precursors indicated by OH reactivity, measurements increased the calculated ozone production potential by as much as $8\,\text{ppb}\,h^{-1}$ (55 %) (Yoshino et al., 2012).

Measurements of OH reactivity provide an upper bound on total VOC oxidation and, in conjunction with measurements of OH concentration, the total RO_2 production rate. Similarly, as HCHO is a major source of HO_2, measurements of HCHO place a lower bound on calculated HO_2 production rates. Correcting for any missing OH reactivity or missing HCHO can increase model XO_2 production rates, in turn increasing $P(O_3)$.

Here, we provide an analysis of HCHO, OH reactivity, and O_3 production using an extensive set of measurements acquired onboard a Zeppelin airship during the Pan-European Gas-AeroSOls Climate Interaction Study (PEGASOS) in the Po Valley region. Through the Zeppelin's slow flight speed, highly spatially and temporally resolved trace gas measurements were acquired (Li et al., 2014). The Zeppelin's unique flight abilities enabled vertical profiling flight tracks from as low as 50 m up to an altitude of ~ 750 m, making possible assessment of the role of exchange between the nocturnal boundary layer, residual layer, and growing mixed layer. In this study, we focus the analysis on one flight for which a clear delineation between those layers occurred (Li et al., 2014). Using a 1-D chemical transport model, we examine the structure and chemical evolution of HCHO vertical profiles. By combining measurements of OH reactivity and VOC precursors, we investigate sources of HCHO in the agricultural regions of the Po Valley. Finally, we discuss the effects of HCHO sources on calculated ozone production rates as a function of time and altitude.

2 Methods

2.1 Zeppelin NT payload and 12 July flight

The Zeppelin NT platform, its scientific payload, and the 12 July flight have been described previously (Li et al., 2014) and are described briefly here. Between 05:30 LT (local time = UTC + 2 h) and 10:45 LT, the airship performed a series of near-surface vertical spirals starting at 50 m and reaching ~ 750 m above sea level (Fig. 1). The airship spiraled upward for ~ 15 min and then returned to lower altitudes within 5 min. The spirals were performed near a ground-based field site at San Pietro Capofiume (SPC, 44°41′ N, 11°38′ E),

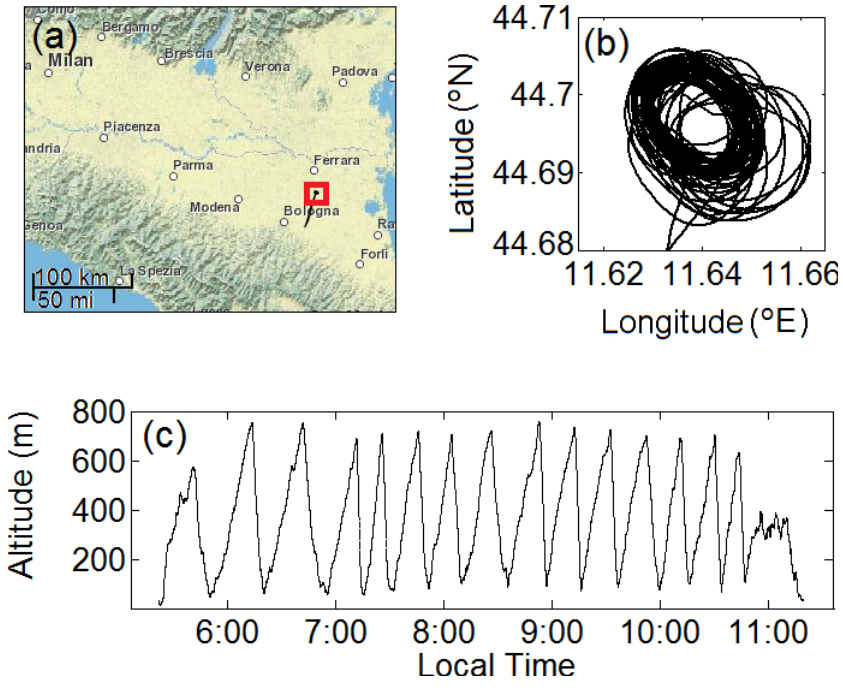

Figure 1. (a) Po Basin, with the 12 July 2012 flight track shown in the box and enlarged in **(b)**. **(c)** Zeppelin altitude during flight.

which is a background urban site according to the European Monitoring and Evaluation Programme (EMEP) criteria (http://www.nilu.no/projects/ccc/manual/). The nearest urban areas include Bologna 25 km to the southwest and Ferrara 20 km to the north. The more immediate region consists primarily of wheat and corn fields that experienced intense harvesting activities during the campaign.

The instrumentation, time resolution, accuracy, and precision of the measurements are fully described in Li et al. (2014) and are summarized here (Table 1). Specifically, HCHO was measured at the Zeppelin nose boom using fiber laser-induced fluorescence (FILIF) (Hottle et al., 2009; DiGangi et al., 2011; Kaiser et al., 2014). The time resolution, precision, and accuracy of the measurement are 1 s, 20–200 ppt, and 15 %, respectively. The 2σ detection limit is 40 ppt. OH reactivity was measured from a platform on top of the Zeppelin by flash photolysis of ozone combined with time-resolved OH detection in a flow tube. The instrument is an improved, more compact version of the instrument described by Lou et al. (2010). The accuracy of the OH reactivity data is 10 %, with a $\pm 0.5\,s^{-1}$ systematic error of the zero-air decay rate coefficients (Gomm, 2014). Speciated C4–C11 VOCs, acetonitrile, and select oxygenated VOCs were measured by a fast gas chromatograph / mass spectrometer system with a time resolution of 180 s and 1σ precision between 3 and 10 % (Jäger, 2014). In addition, OH, HO_2, NO, NO_2, O_3, CO, HONO, particle concentration/size distribution, solar actinic flux densities, temperature, pressure, relative humidity, and 3-D wind were measured simultaneously.

2.2 Model simulations

The Chemistry of Atmosphere-Forest Exchange (CAFE) model is a 1-D chemical transport model that has previously been used in steady-state analysis of trace gas fluxes above a pine forest (Wolfe and Thornton, 2011; Wolfe et al., 2011). For this study, the CAFE framework has been adapted to run in a time-dependent manner and, as the region is not forested, no canopy structure is included. The chemical mechanism generated by the Master Chemical Mechanism (MCM) v3.2 (Jenkin et al., 1997; Saunders et al., 2003; Bloss et al., 2005) contains near-explicit degradation schemes for all constrained VOCs as well as all relevant inorganic chemistry (more information available at http://mcm.leeds.ac.uk/MCM). The model was run with seven evenly spaced altitude bins, with altitudes from 50 to 150 m for the lowest box and from 650 to 750 m for the highest box. Measurements acquired during Zeppelin ascents were averaged into these 100 m altitude bins. Because descents were performed much more quickly than ascents, data acquired during the ascents have a higher spatial resolution than descent data. Where instrument time resolution limits data availability, concentrations are interpolated from data at surrounding altitude and time bins. In all model scenarios, measured photolysis frequencies are used where available. Otherwise, MCM calculated values are scaled according to the ratio of the calculated and measured photolysis rates of NO_2.

While methane was not measured at the SPC ground site or from the Zeppelin, measurements of CH_4 were acquired from a mobile aerosol and trace gas laboratory

Table 1. Zeppelin-based measurements used for the analysis of O_3 and HCHO production.

Parameter	Technique	Precision (1σ)	Accuracy
HCHO	FILIF[a]	20–200 ppt/s	15 %
HONO	LOPAP[b]	1.3 ppt/180 s	12 %
OH	Laser-induced fluorescence[c]	Day LOD: 1.3×10^6 cm^{-3}/42 s Night LOD: 0.67×10^6 cm^{-3}/42 s	14 %
HO_2	Laser-induced fluorescence[d]	Day LOD: 81×10^6 cm^{-3}/42 s Night LOD: 36×10^6 cm^{-3}/42 s	24–30 %
OH reactivity	Laser-induced fluorescence[e]	6 %/2 min (standard deviation)	10 %
NO	Chemiluminescence[f]	10 ppt/60 s	5 %
NO_2	Conversion to NO[g] followed by chemiluminescence[f]	30 ppt/60 s	7.5 %
O_3	UV absorption[h]	1 ppb/20 s	3 %
CO	Resonance fluorescence[i]	5 ppb/1 s	5 %
VOCs	Fast GC/MS[j]	3–10 %/180 s	15 %
Photolysis frequencies	Spectroradiometer[k]	$-$(1 s)[k]	15 %[k]
Relative humidity	Vaisala HUMICAP HMP45	0.1 % RH/1 s	2 % RH
Temperature	PT100	0.1 °C/1 s	0.1 °C
Pressure	Barometric SETRA	< 0.5 mbar/1 s	33 mbar

[a]Fiber laser-induced fluorescence (Hottle et al., 2009). [b]Long path absorption photometry (Li et al., 2014). [c]Holland et al. (2003). [d]Fuchs et al. (2011). [e]Lou et al. (2010). [f]ECOPHYSICS (type TR780). [g]Photolytic blue light converter (Droplet Technologies type BLC). [h]ENVIRONNEMENT S.A (type O342M). [i]Gerbig et al. (1999). [j]Gas chromatography/mass spectrometry (Jäger, 2014). [k]Bohn et al. (2008). Accuracy and precision are dependent on conditions and the photolysis process. The 15 % accuracy is a conservative estimate covering important photolysis frequencies.

(Measurements Of Spatial QUantitative Immissions of Trace gases and Aerosols: MOSQUITA; Bukowiecki et al., 2002; Mohr et al., 2011), which was equipped with a Picarro cavity ring-down spectroscopy analyzer (model G2401). MOSQUITA-based CH_4 measurements were acquired from 8 June 2012 to 9 July 2012. Though measurements are not available for the day of the flight studied here, the average measurement acquired in the flight region of the Zeppelin (2355 ppb) is likely applicable to this study.

In the base case scenario, the model is constrained to all measurements, with the exception of HCHO. Given the extensive constraints, deposition, emission, and advection are not treated explicitly. Because deposition can be a non-negligible sink for many oxidized species (including HCHO), model results represent an upper limit on calculated mixing ratios. Turbulent diffusion is represented using K-theory, where diffusion coefficients are calculated using the single-column chemistry and climate model ECHAM4(SCM) (Ganzeveld et al., 2002). Further discussion of the eddy diffusion coefficient, uncertainty associated with turbulent diffusion, and the potential influence of deposition is available in the Supplement.

To initialize non-measured species (e.g., speciated RO_2 and organic nitrates), a "spin-up" 0-D diurnal model run was performed constraining all species to a combination of the lowest altitude Zeppelin measurements and available measurements from the nearby SPC ground site acquired between 12 June and 10 July 2012. This includes average diurnal profiles of CO, O_3, benzene, toluene, NO_x, and relevant meteorological parameters. An average methane concentration of 2355 ppb from the MOSQUITA mobile laboratory was assumed. Anthropogenic VOCs were scaled to ground benzene measurements according to their observed relationship with benzene measurements acquired on the Zeppelin. To mimic the temperature dependence of isoprene emission rates, isoprene mixing ratios were assumed to be proportional to the cosine of the solar zenith angle and scaled to available Zeppelin measurements. As isoprene concentrations are small (< 100 ppt), the diurnal cycle has a negligible impact on modeled results. For 1-D model simulations, non-measured species are initialized to the output of the spin-up model at 06:00 LT on the fourth day scaled to HCHO measured on the Zeppelin as a function of altitude.

3 Results and discussion

3.1 Observed HCHO and OH reactivity

In the following section, we present observations of HCHO, VOCs, and OH reactivity acquired on the 12 July flight in the context of previous Po Valley measurements. A detailed presentation of additional trace gas measurements (notably HONO, NO_x, O_3, HO_2, and H_2O) as well as a discussion of

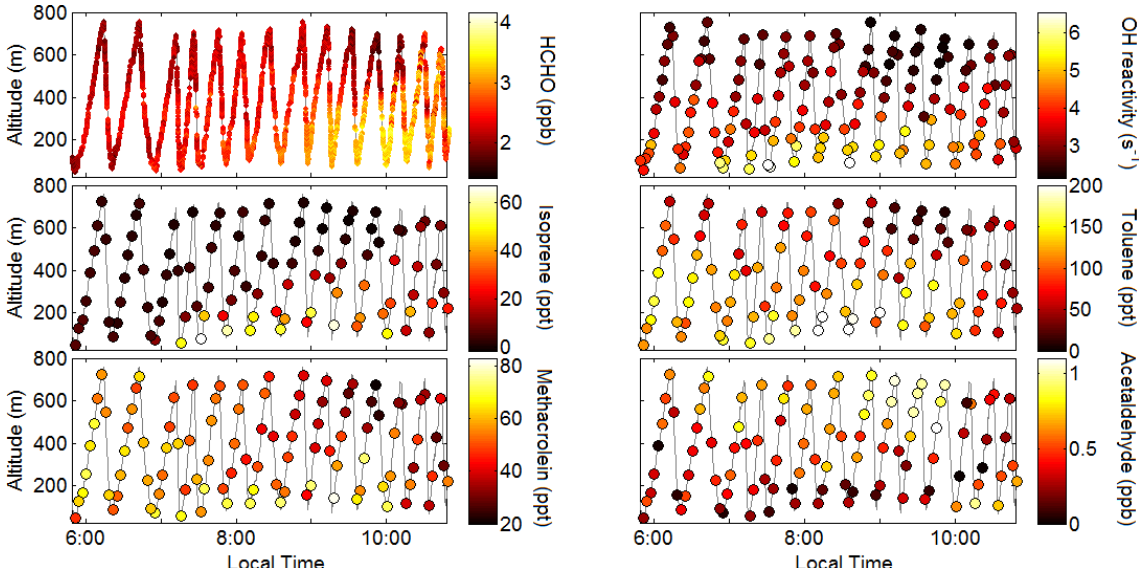

Figure 2. Flight pattern colored by selected measurements.

the delineation between the residual layer, nocturnal boundary layer, and mixed layer can be found in Li et al. (2014).

Figure 2 shows measured HCHO, OH reactivity, and selected VOCs as a function of time and altitude. Primary biogenic VOC concentrations were low throughout the entire flight (isoprene < 60 ppt), which is consistent with previous measurements at Verzago, an agriculture site downwind of Milan (Steinbacher et al., 2005a). Anthropogenic VOCs such as toluene and benzene were around an order of magnitude lower than at Verzago in 2003 (Steinbacher et al., 2005b). In contrast to primary biogenic and anthropogenic VOCs, oxidized VOCs were abundant (reaching HCHO > 3.8 ppb, acetaldehyde > 1.0 ppb). The overall magnitude and morning rise of HCHO observed were similar to those observed previously in Spessa in 2002 (Junkermann, 2009).

Before sunrise, elevated levels of toluene and other anthropogenic VOCs were observed in the residual layer compared to lower altitudes. Accumulation of VOC oxidation products including HCHO, methacrolein, and acetaldehyde was observed in the nocturnal boundary and in the residual layer. These oxidation products are either built up overnight or remain elevated from the previous day. After sunrise (05:45 LT), both biogenic and anthropogenic primary VOC increase in the developing mixed layer. The observed increase in HCHO mixing ratios lags that of primary VOCs, so that higher HCHO concentrations were observed ∼ 4 h after sunrise. The general vertical structure of the observed OH reactivity tracks well with HCHO, with elevated values in nocturnal boundary and growing mixed layers. Based on the vertical structure of the observed HCHO and other trace gasses, potential sources of HCHO are discussed further in Sect. 3.3.

3.2 Base scenario modeled OH reactivity and HCHO

The top panel of Fig. 3 shows the measured and modeled OH reactivity as a function of time and altitude. Overall, the magnitude and vertical structure is well captured by measured VOCs and their oxidation products. Where underestimated, the average discrepancy is less than 7 %, with larger discrepancies at lower altitudes. Speciated model contributions to OH reactivity are shown in Fig. 4, calculated with all species (including HCHO) constrained to observations. Largely, NO_x dominates the modeled OH reactivity, contributing 40 % to modeled reactivity at 100 m and 08:45 LT. The contribution of measured VOCs and OVOCs is most significant in the mixed layer (26 % at 100 m, 08:45 LT). HCHO consistently contributes the largest portion of calculated OH reactivity (HCHO reactivity ∼ 0.2 s^{-1} ppb^{-1}, 8 % of total modeled reactivity at 100 m and 08:45 LT).

Figure 3 also shows measured and modeled HCHO. Before 09:00 LT, base case modeled HCHO matches measurements quite well. This is expected, as the model is initialized to measure HCHO mixing ratios, and low OH concentrations as well as a lack of photolysis lead to very little change. Model/measurement discrepancy grows with time and is largest at low altitudes. Between 06:32 and 10:06 LT, HCHO increases by as much as 1.3 ppb, while the model predicts no net increase. HCHO loss terms are unlikely to be overestimated, as they are constrained by measured OH and measured HCHO photolysis frequencies, and could potentially be underestimated by neglecting deposition (see the Supplement). This finding implies that the model is missing either chemical HCHO production, advection of HCHO, or a local source of direct HCHO emissions.

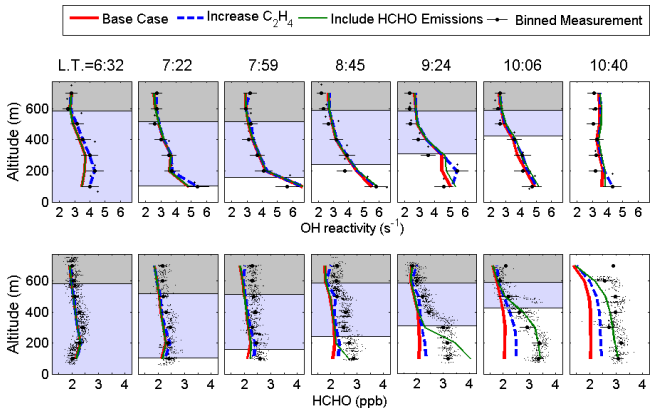

Figure 3. Measured and calculated OH reactivity and HCHO vertical profiles for every other Zeppelin ascent. Error bars on OH reactivity represent the measurement precision. Error bars on HCHO represent the standard deviation of the measurements in the given altitude bin. The gray, blue, and white areas represent the residual layer, the nocturnal boundary layer, and the mixed layer, respectively. Layer height was determined by the observed steep gradients in O_3 mixing ratios, as detailed in Li et al. (2014). Model scenarios are described in more detail in Sects. 3.2 and 3.3.

3.3 Potential sources of HCHO

The oxidation of additional non-measured VOCs is often cited as a possible source of missing HCHO production in models (compared to the FORMAT study; Junkermann, 2009). Using OH reactivity measurements, one can place an upper bound on the overall VOC oxidation rate in the atmosphere. As discussed above, measured VOCs and their modeled oxidation products explain the majority of observed OH reactivity, though a small discrepancy is occasionally observed. To investigate the possibility of non-measured HCHO precursors, an additional model scenario is constructed in which the missing OH reactivity is assumed to be comprised entirely of ethene (C_2H_4). C_2H_4 was chosen as a surrogate species because it produces HCHO from OH and O_3 oxidation with respective yields of 160 % (Niki et al., 1981) and 154 % (Alam et al., 2011). Thus, the increase in modeled HCHO per increase in calculated OH reactivity is maximized.

Figure 3 shows the effect of increasing C_2H_4 on HCHO and OH reactivity. While measured mixed-layer HCHO increases by as much as 1.3 ppb between 06:30 and 10:00 LT, model HCHO increases by only 300 ppt. In order to generate the required HCHO, modeled C_2H_4 would need to be increased such that calculated OH reactivity is up to 56 % greater than the measurements. While the model vertical profile at 10:40 LT is in better agreement with measurements, at the 09:24 LT vertical profile, additional VOC precursors can explain no more than 0.26 ppb, or 23 %, of the missing HCHO budget. We therefore conclude that non-measured VOCs cannot explain the discrepancy in measured and modeled HCHO.

Another possible source of HCHO is transport from nearby urban centers. In the early morning, the average wind speed was less than 1.2 m s^{-1}, and the average HCHO lifetime was $\sim$ 3.5 h. Between 06:00 and 10:30 LT, the bottommost layer in contact with the surface grows from less than 50 m to more than 600 m in height. Accounting for this dilution, and the HCHO lifetime and wind speed, and assuming a nighttime concentration in Bologna of 6 ppb (near the maximum nocturnal concentration reported in Milan; Junkermann, 2009), the amount of HCHO advected could be no more than 90 ppt, or 7 % of the missing HCHO budget. Additionally, no other long-lived tracers of anthropogenic influence (i.e., CO, xylenes) show a rise in the late morning. Finally, the vertical profile of the missing HCHO suggests a strong source near the ground, which is convectively incorporated into the growing mixed layer. As advection of HCHO, e.g., from Bologna, would more likely affect the mixed layer as a whole, transport is an unlikely source of HCHO.

As the air aloft initially has slightly elevated levels of HCHO, entrainment of air from the residual layer into the mixed layer is an additional potential source of HCHO. Using ECHAM4(SCM) to investigate observations from the October 2005 field campaign over the Atlantic Ocean, French Guyana, and Suriname, Ganzeveld et al. (2008) demonstrated that the assessment of daytime HCHO requires a thorough evaluation of the morning turbulent transport. The model-predicted entrainment of HCHO would affect the daytime radical budget and resulting oxidative chemistry; however, limited observations in the residual layer did not allow for comparison of SCM simulations with measurements. If entrainment was the primary cause of measurement and model discrepancy, the missing HCHO would be larger near the top of the boundary layer and when HCHO concentrations aloft are the highest. In this study, the largest discrepancies occur at the lowest altitudes and later in the morning. The highly resolved vertical measurements enabled by the Zeppelin aircraft demonstrate that, for this study, entrainment is unlikely to be the primary cause of model/measurement discrepancies at low altitudes.

An additional potential source of HCHO is local direct emission from biomass burning or other anthropogenic activities. Aircraft measurements in 2003 showed evidence of biomass burning contribution to elevated HCHO in the agricultural regions of the Po Valley (Junkermann, 2009); however, these measurements were in September and October after the harvesting of the rice fields, and we did not see such strong local sources during the flight. Acetonitrile, a tracer of biomass burning, remains at a background level of less than 250 ppt. As CO is a product of incomplete fuel combustion, it can be used to trace the influence of local traffic. CO does not increase significantly during the time HCHO increases in the mixed layer (Fig. 5). Using an emission ratio of 3.14 g HCHO kg^{-1} CO observed at a highway junction in

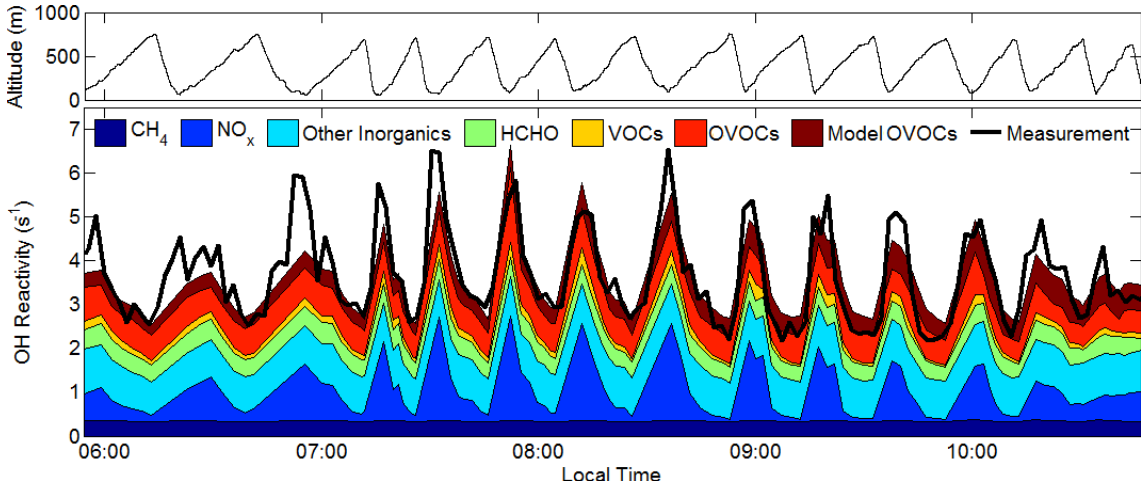

Figure 4. Contributions to calculated OH reactivity as a function of time. Only data acquired during the ascents are used in the calculated reactivity. The VOC category consists of isoprene, toluene, benzene, xylenes, ethylbenzene, C4–C9 straight chain alkanes, styrene, trimethylbenzene, 1-pentene, cis-2-pentene, cyclohexanone, propylbenzene, isopropylbenzene, isopentane, benzaldehyde, and 1-butene. The OVOC category consists of C2–C6 straight chain aldehydes, acetone, methanol, ethanol, methyl acetate, ethyl acetate, methacrolein, methyl ethyl ketone, methyl vinyl ketone, and 1-propanol. The inorganics category consists of CO, H_2, HONO, HO_2, and O_3. Model OVOCs are non-measured oxidation products calculated by the MCM.

Houston, Texas (Rappenglueck et al., 2013), the increase of 19 ppb in CO between 06:20 and 10:00 LT, if wholly from traffic emissions, could account for only 57 ppt (4 %) of the observed increase in HCHO. We therefore conclude that neither biomass burning nor traffic can account for the relatively high levels of observed HCHO.

Finally, the soil, decaying plant matter from harvesting, or wheat or other crops in the region of the Zeppelin spirals may be a source of local direct HCHO emission. Measurements of oxygenated VOCs (OVOCs) from agricultural crops are limited. Konig et al. (1995) reported that total OVOC emission rates from wheat were $10.9\,\mathrm{ng\,g^{-1}\,h^{-1}}$, though speciated measurements of formaldehyde were not available. Dry weight HCHO emission rates from tree species in Italy are much higher, ranging from 382 to $590\,\mathrm{ng\,g^{-1}\,h^{-1}}$ (Kesselmeier et al., 1997). Oxygenated VOC emissions are expected to respond differently to light and temperature than terpenoids (Rinne et al., 2007); nevertheless, the classic terpenoid exponential model is often extended to OVOC emissions. For example, for ground emissions of HCHO in a ponderosa pine forest, DiGangi et al. (2011) applied an emission algorithm of $E_{\mathrm{HCHO}} = A \cdot \exp(\beta T)$, where $A = 740\,\mathrm{ng\,m^{-2}\,h^{-1}}$ and $\beta = 0.07\,^{\circ}\mathrm{C}^{-1}$. The emissions were scaled by photosynthetically active radiation, with night-time emissions fixed to 15 % of daytime emissions.

A final model scenario was constructed that incorporates direct emissions of HCHO according to the sunlight-weighted exponential emission function similar to DiGangi et al. (2011), employing a much smaller prefactor of $A = 375\,\mathrm{ng\,m^{-2}\,h^{-1}}$ to best capture the observed HCHO mixing ratios. These emissions are added as a direct HCHO source for the model's surface layer (0–50 m), with all other surface layer concentrations constrained to their lowest altitude measurement. The results are shown in Fig. 3. The vertical profile is mostly consistent with measurements, with possible discrepancies arising from uncertainty in eddy diffusion constants (see Supplement). Due to the good agreement of this model result and the improbability of other HCHO sources, we conclude that local direct emissions from agricultural land are the most likely source of additional HCHO.

The finding that direct biogenic emission could account for a large percentage of the observed increase in the HCHO mixing ratio is in contrast with the Liu et al. (2007) assumption that direct emissions account for only ∼ 10 % of HCHO sources in the agricultural Po Valley. Due to scarce data availability, limited information on chemical speciation, and only rough estimates of emission rates, models often assume a default emission rate for all oxygenated VOCs independent of land use or plant type (Karl et al., 2009). To realize the full potential of these oxidized VOCs as tracers of the photochemistry that forms secondary pollutants, and to understand their effects on such chemistry, thorough studies of direct emission are needed.

3.4 Implications for ozone production

An additional HCHO source, regardless of the type, will have a direct impact on calculated ozone production rates. The in situ ozone production can be calculated as

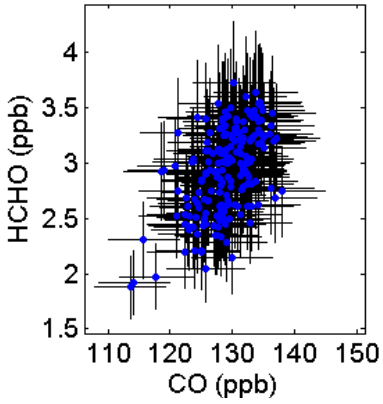

Figure 5. HCHO and CO in the mixed layer. Error bars represent instrument accuracy. There is little variation in mixed layer CO, and the correlation with HCHO is low ($r^2 = 0.29$).

$$P(O_3) = k_{HO_2+NO}[HO_2][NO] + \sum_i k_{RO_2i+NO}[RO_{2i}][NO], \quad (2)$$

where NO_2 is assumed to photodissociate, leading to immediate ozone production (reactions 1 and 2). In our MCM-based calculations, the formation of organic nitrates is accounted for in the $RO_2 + NO$ reaction rates. As direct measurements of RO_2 were not available on the Zeppelin, the analysis presented here relies on speciated modeled RO_2 concentrations and reaction rates. Typical model RO_2 concentrations are between 10 and 30 % of the sum of modeled RO_2 and measured HO_2, such that HO_2 accounts for the majority of the modeled NO to NO_2 conversion. Because HCHO photolysis and oxidation account for as much as 39 % of model HO_2 production, failing to include all sources of HCHO has significant effects on calculated HO_2 concentrations. Though not probable in this analysis, if oxidation of unmeasured VOCs contributes significantly to the HCHO budget, RO_2 concentrations would likely be underestimated.

Because the effects of transport on O_3 may be large, we do not explicitly compare measured and modeled O_3 concentrations in this study. Instead, two model scenarios were constructed to estimate the impact of missing HCHO on HO_2 mixing ratios and therefore ozone production. Both simulations were carried out with HO_2 unconstrained, and HCHO was either fixed to observations or calculated by the model. Constraining HO_2 has a negligible effect on modeled HCHO concentrations. Because the difference in the concentration of HO_2 between the two model scenarios is smaller than the measurement uncertainty (~ 12 % compared to 30 %), and because both model scenarios reproduce HO_2 concentration within the measurement uncertainty, measured and modeled HO_2 are not compared. At the observed mixed layer NO concentrations of ~ 1 ppb and a rate constant of

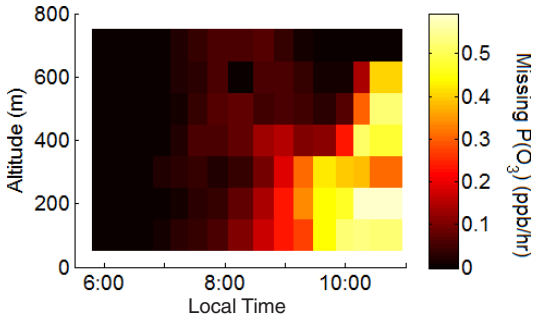

Figure 6. Underestimate in ozone production rate caused by the modeled underestimate in HCHO as a function of time and altitude. Missing $P(O_3)$ is defined as $P(O_3)$ calculated using measured HCHO minus $P(O_3)$ calculated using modeled HCHO.

$k_{HO_2+NO} = 8.6 \times 10^{-12}$ cm^3 molec^{-1} s^{-1}, an increase of just 1 ppt HO_2 corresponds to an additional 0.7 ppb h^{-1} (14 %) of ozone production. Figure 6 shows the difference in $P(O_3)$ driven by differences in calculated HO_2 concentrations. Assuming that the trend in the discrepancy in HCHO will continue to increase throughout the day, an increasing underprediction of the local ozone production rate is expected for this agricultural region.

4 Conclusions

Using a near-explicit 1-D model and a comprehensive set of trace gas measurements acquired from a Zeppelin airship, we have examined VOC oxidation and its relationship to ozone production in the Po Valley. As in previous work in the region, our model was largely unable to reproduce the morning rise and high levels of observed HCHO. Measured OH reactivity, however, was explained by measured VOCs and their calculated oxidation products. The most probable source of missing HCHO is direct emission from the soil and plant matter beneath the Zeppelin. As a result of the underestimate in HCHO, model ozone production rates based on HO_2 concentrations are underestimated by as much as 12 % before noon, and the underestimate is expected to increase. When considering photochemical models of O_3 production, even small underestimates in HCHO can lead to large underestimates of local ozone production rates. For that reason, and considering the large portion of land used globally for similar agricultural purposes, direct measurements of OH reactivity and HCHO as well as improved OVOC emission inventories would aid in the prediction of high ozone events.

The Supplement related to this article is available online at doi:10.5194/acp-15-1289-2015-supplement.

Acknowledgements. This work is within the PEGASOS project, which is funded by the European Commission under Framework Programme 7 (FP7-ENV-2010-265148). The authors would like to acknowledge all members of the PEGASOS flight and science teams. We also acknowledge Zeppelin Luftschifftechnik (ZLT) and Deutsche Zeppelin Reederei (DZR) for their cooperation. J. Jäger, R. Wegener, I. Lohse, and B. Bohn would like to thank the Deutsche Forschungsgemeinschaft for funding within priority program HALO (WE-4384/2-2 and BO1580/4-1). J. Kaiser, G. M. Wolfe, and F. Keutsch would like to thank Maria Cazorla for helping with the calibration of the HCHO measurements and NSF-AGS (1051338) and Forschungszentrum Jülich for support. G. Wolfe acknowledges support from the NOAA Climate and Global Change Postdoctoral Fellowship Program. J. Kaiser acknowledges support from the National Science Foundation Graduate Research Fellowship Program under grant no. DGE-1256259. We would like to thank ARPA Emilia-Romagna (Region Agency for Environmental Protection in the Emilia-Romagna region Italy) and all participants in the Supersito Project for providing measurements at the SPC ground site. The authors also acknowledge Christos Kaltsonoudis and Spyros Pandis from the Laboratory of Air Quality Studies at the University of Patras for making CO data from the SPC ground site available.

Edited by: E. Nemitz

References

Alam, M. S., Camredon, M., Rickard, A. R., Carr, T., Wyche, K. P., Hornsby, K. E., Monks, P. S., and Bloss, W. J.: Total radical yields from tropospheric ethene ozonolysis, Phys. Chem. Chem. Phys., 13, 11002–11015, doi:10.1039/c0cp02342f, 2011.

Bloss, C., Wagner, V., Jenkin, M. E., Volkamer, R., Bloss, W. J., Lee, J. D., Heard, D. E., Wirtz, K., Martin-Reviejo, M., Rea, G., Wenger, J. C., and Pilling, M. J.: Development of a detailed chemical mechanism (MCMv3.1) for the atmospheric oxidation of aromatic hydrocarbons, Atmos. Chem. Phys., 5, 641–664, doi:10.5194/acp-5-641-2005, 2005.

Bohn, B., Corlett, G. K., Gillmann, M., Sanghavi, S., Stange, G., Tensing, E., Vrekoussis, M., Bloss, W. J., Clapp, L. J., Kortner, M., Dorn, H.-P., Monks, P. S., Platt, U., Plass-Dülmer, C., Mihalopoulos, N., Heard, D. E., Clemitshaw, K. C., Meixner, F. X., Prevot, A. S. H., and Schmitt, R.: Photolysis frequency measurement techniques: results of a comparison within the ACCENT project, Atmos. Chem. Phys., 8, 5373–5391, doi:10.5194/acp-8-5373-2008, 2008.

Bukowiecki, N., Dommen, J., Prévôt, A. S. H., Richter, R., Weingartner, E., and Baltensperger, U.: A mobile pollutant measurement laboratory – measuring gas phase and aerosol ambient concentrations with high spatial and temporal resolution, Atmos. Environ., 36, 5569–5579, doi:10.1016/S1352-2310(02)00694-5, 2002.

DiGangi, J. P., Boyle, E. S., Karl, T., Harley, P., Turnipseed, A., Kim, S., Cantrell, C., Maudlin III, R. L., Zheng, W., Flocke, F., Hall, S. R., Ullmann, K., Nakashima, Y., Paul, J. B., Wolfe, G. M., Desai, A. R., Kajii, Y., Guenther, A., and Keutsch, F. N.: First direct measurements of formaldehyde flux via eddy covariance: implications for missing in-canopy formaldehyde sources, Atmos. Chem. Phys., 11, 10565–10578, doi:10.5194/acp-11-10565-2011, 2011.

Dolgorouky, C., Gros, V., Sarda-Esteve, R., Sinha, V., Williams, J., Marchand, N., Sauvage, S., Poulain, L., Sciare, J., and Bonsang, B.: Total OH reactivity measurements in Paris during the 2010 MEGAPOLI winter campaign, Atmos. Chem. Phys., 12, 9593–9612, doi:10.5194/acp-12-9593-2012, 2012.

Edwards, P. M., Evans, M. J., Furneaux, K. L., Hopkins, J., Ingham, T., Jones, C., Lee, J. D., Lewis, A. C., Moller, S. J., Stone, D., Whalley, L. K., and Heard, D. E.: OH reactivity in a South East Asian tropical rainforest during the Oxidant and Particle Photochemical Processes (OP3) project, Atmos. Chem. Phys., 13, 9497–9514, doi:10.5194/acp-13-9497-2013, 2013.

Fuchs, H., Bohn, B., Hofzumahaus, A., Holland, F., Lu, K. D., Nehr, S., Rohrer, F., and Wahner, A.: Detection of HO_2 by laser-induced fluorescence: calibration and interferences from RO_2 radicals, Atmos. Meas. Tech., 4, 1209–1225, doi:10.5194/amt-4-1209-2011, 2011.

Ganzeveld, L., Lelieveld, J., Dentener, F., Krol, M., and Roelofs, G.: Atmosphere-biosphere trace gas exchanges simulated with a single-column model, J. Geophys. Res.-Atmos., 107, ACH8.1–ACH8.21, doi:10.1029/2001JD000684, 2002.

Ganzeveld, L., Eerdekens, G., Feig, G., Fischer, H., Harder, H., Königstedt, R., Kubistin, D., Martinez, M., Meixner, F. X., Scheeren, H. A., Sinha, V., Taraborrelli, D., Williams, J., Vilà-Guerau de Arellano, J., and Lelieveld, J.: Surface and boundary layer exchanges of volatile organic compounds, nitrogen oxides and ozone during the GABRIEL campaign, Atmos. Chem. Phys., 8, 6223–6243, doi:10.5194/acp-8-6223-2008, 2008.

Gerbig, C., Schmitgen, S., Kley, D., Volz-Thomas, A., Dewey, K., and Haaks, D.: An improved fast-response vacuum-UV resonance fluorescence CO instrument, J. Geophys. Res., 104, 1699–1704, doi:10.1029/1998JD100031, 1999.

Gomm, S.: Luftgestützte Messung von HOx-Radikalkonzentrationen mittels Laser-induzierter Fluoreszenz auf einem Zeppelin NT: Untersuchung der atmosphärischen Oxidationsstärke der unteren Troposphäre, PhD, Bergische-Universität Wuppertal, 2014.

Holland, F., Hofzumahaus, A., Schäfer, R., Kraus, A., and Pätz, H. W.: Measurements of OH and HO_2 radical concentrations and photolysis frequencies during BERLIOZ, J. Geophys. Res.-Atmos., 108, PHO2.1–PHO2.23, doi:10.1029/2001jd001393, 2003.

Hottle, J., Huisman, A., Digangi, J., Kammrath, A., Galloway, M., Coens, K., and Keutsch, F.: A Laser Induced Fluorescence-Based Instrument for In-Situ Measurements of Atmospheric Formaldehyde, Environ. Sci. Technol., 43, 790–795, doi:10.1021/es801621f, 2009.

Jäger, J.: Airborne VOC measurements on board the Zeppelin NT during PEGASOS campaigns in 2012 deploying the improved Fast-GC-MSD System, PhD, Forschungszentrum Jülich GmbH, Jülich, Germany, 2014.

Jenkin, M., Saunders, S., and Pilling, M.: The tropospheric degradation of volatile organic compounds: A protocol for mechanism development, Atmos. Environ., 31, 81–104, doi:10.1016/S1352-2310(96)00105-7, 1997.

Junkermann, W.: On the distribution of formaldehyde in the western Po-Valley, Italy, during FORMAT 2002/2003, Atmos. Chem. Phys., 9, 9187–9196, doi:10.5194/acp-9-9187-2009, 2009.

Kaiser, J., Li, X., Tillmann, R., Acir, I., Holland, F., Rohrer, F., Wegener, R., and Keutsch, F. N.: Intercomparison of Hantzsch and fiber-laser-induced-fluorescence formaldehyde measurements, Atmos. Meas. Tech., 7, 1571–1580, doi:10.5194/amt-7-1571-2014, 2014.

Karl, M., Guenther, A., Köble, R., Leip, A., and Seufert, G.: A new European plant-specific emission inventory of biogenic volatile organic compounds for use in atmospheric transport models, Biogeosciences, 6, 1059–1087, doi:10.5194/bg-6-1059-2009, 2009.

Kesselmeier, J., Bode, K., Hofmann, U., Muller, H., Schafer, L., Wolf, A., Ciccioli, P., Brancaleoni, E., Cecinato, A., Frattoni, M., Foster, P., Ferrari, C., Jacob, V., Fugit, J. L., Dutaur, L., Simon, V., and Torres, L.: Emission of short chained organic acids, aldehydes and monoterpenes from Quercus ilex L. and Pinus pinea L. in relation to physiological activities, carbon budget and emission algorithms, Atmos. Environ., 31, 119–133, doi:10.1016/s1352-2310(97)00079-4, 1997.

Konig, G., Brunda, M., Puxbaum, H., Hewitt, C. N., Duckham, S. C., and Rudolph, J.: Relative contribution of oxygenated hydrocarbons to the total biogenic VOC emissions of selected Mid-European agricultural and natural plant-species, Atmos. Environ., 29, 861–874, doi:10.1016/1352-2310(95)00026-u, 1995.

Li, X., Rohrer, F., Hofzumahaus, A., Brauers, T., Häseler, R., Bohn, B., Broch, S., Fuchs, H., Gomm, S., Holland, F., Jäger, J., Kaiser, J., Keutsch, F. N., Lohse, I., Lu, K., Tillmann, R., Wegener, R., Wolfe, G. M., Mentel, T. F., Kiendler-Scharr, A., and Wahner, A.: Missing Gas-Phase Source of HONO Inferred from Zeppelin Measurements in the Troposphere, Science, 344, 292–296, doi:10.1126/science.1248999, 2014.

Liu, L., Andreani-Aksoyoglu, S., Keller, J., Ordonez, C., Junkermann, W., Hak, C., Braathen, G., Reimann, S., Astorga-Llorens, C., Schultz, M., Prevot, A., and Isaksen, I.: A photochemical modeling study of ozone and formaldehyde generation and budget in the Po basin, J. Geophys. Res.-Atmos., 112, D22303, doi:10.1029/2006JD008172, 2007.

Lou, S., Holland, F., Rohrer, F., Lu, K., Bohn, B., Brauers, T., Chang, C. C., Fuchs, H., Häseler, R., Kita, K., Kondo, Y., Li, X., Shao, M., Zeng, L., Wahner, A., Zhang, Y., Wang, W., and Hofzumahaus, A.: Atmospheric OH reactivities in the Pearl River Delta – China in summer 2006: measurement and model results, Atmos. Chem. Phys., 10, 11243–11260, doi:10.5194/acp-10-11243-2010, 2010.

Mohr, C., Richter, R., DeCarlo, P. F., Prévôt, A. S. H., and Baltensperger, U.: Spatial variation of chemical composition and sources of submicron aerosol in Zurich during wintertime using mobile aerosol mass spectrometer data, Atmos. Chem. Phys., 11, 7465–7482, doi:10.5194/acp-11-7465-2011, 2011.

Niki, H., Maker, P. D., Savage, C. M., and Breitenbach, L. P.: An FTIR study of mechanisms for the HO radical initiated oxidation of C_2H_4 in the presence of NO: Detection of glycolaldehyde, Chem. Phys. Lett., 80, 499–503, 1981.

Rappenglueck, B., Lubertino, G., Alvarez, S., Golovko, J., Czader, B., and Ackermann, L.: Radical precursors and related species from traffic as observed and modeled at an urban highway junction, JAPCA J. Air Waste Ma., 63, 1270–1286, doi:10.1080/10962247.2013.822438, 2013.

Rinne, J., Taipale, R., Markkanen, T., Ruuskanen, T. M., Hellén, H., Kajos, M. K., Vesala, T., and Kulmala, M.: Hydrocarbon fluxes above a Scots pine forest canopy: measurements and modeling, Atmos. Chem. Phys., 7, 3361–3372, doi:10.5194/acp-7-3361-2007, 2007.

Sadanaga, Y., Yoshino, A., Kato, S., and Kajii, Y.: Measurements of OH reactivity and photochemical ozone production in the urban atmosphere, Environ. Sci. Technol., 39, 8847–8852, doi:10.1021/es049457p, 2005.

Saunders, S. M., Jenkin, M. E., Derwent, R. G., and Pilling, M. J.: Protocol for the development of the Master Chemical Mechanism, MCM v3 (Part A): tropospheric degradation of non-aromatic volatile organic compounds, Atmos. Chem. Phys., 3, 161–180, doi:10.5194/acp-3-161-2003, 2003.

Steinbacher, M., Dommen, J., Ordonez, C., Reimann, S., Gruebler, F., Staehelin, J., Andreani-Aksoyoglu, S., and Prevot, A. S. H.: Volatile organic compounds in the Po Basin. part B: Biogenic VOCs, J. Atmos. Chem., 51, 293–315, doi:10.1007/s10874-005-3577-0, 2005a.

Steinbacher, M., Dommen, J., Ordonez, C., Reimann, S., Gruebler, F. C., Staehelin, J., and Prevot, A. S. H.: Volatile organic compounds in the Po Basin. part A: Anthropogenic VOCs, J. Atmos. Chem., 51, 271–291, doi:10.1007/s10874-005-3576-1, 2005b.

Wolfe, G. M. and Thornton, J. A.: The Chemistry of Atmosphere-Forest Exchange (CAFE) Model – Part 1: Model description and characterization, Atmos. Chem. Phys., 11, 77–101, doi:10.5194/acp-11-77-2011, 2011.

Wolfe, G. M., Thornton, J. A., Bouvier-Brown, N. C., Goldstein, A. H., Park, J.-H., McKay, M., Matross, D. M., Mao, J., Brune, W. H., LaFranchi, B. W., Browne, E. C., Min, K.-E., Wooldridge, P. J., Cohen, R. C., Crounse, J. D., Faloona, I. C., Gilman, J. B., Kuster, W. C., de Gouw, J. A., Huisman, A., and Keutsch, F. N.: The Chemistry of Atmosphere-Forest Exchange (CAFE) Model – Part 2: Application to BEARPEX-2007 observations, Atmos. Chem. Phys., 11, 1269–1294, doi:10.5194/acp-11-1269-2011, 2011.

Yoshino, A., Nakashima, Y., Miyazaki, K., Kato, S., Suthawaree, J., Shimo, N., Matsunaga, S., Chatani, S., Apel, E., Greenberg, J., Guenther, A., Ueno, H., Sasaki, H., Hoshi, J., Yokota, H., Ishii, K., and Kajii, Y.: Air quality diagnosis from comprehensive observations of total OH reactivity and reactive trace species in urban central Tokyo, Atmos. Environ., 49, 51–59, doi:10.1016/j.atmosenv.2011.12.029, 2012.